JOURNAL OF MOLECULAR SPECTROSCOPY 172, 233–242 (1995)

Frequency Measurements and Molecular Constants of CO_2 00^02–$[10^01,02^01]_{I,II}$ Sequence Band Transitions

CHE-CHUNG CHOU,* A. G. MAKI,† S. JA. TOCHITSKY,*,[1] JOW-TSONG SHY,* K. M. EVENSON,‡ AND L. R. ZINK‡

Department of Physics, National Tsing Hua University, Hsinchu, Taiwan 30043, Republic of China; †15012 24 Ave. S. E., Mill Creek, Washington 98012-5718; and ‡Time and Frequency Division, National Institute of Standards and Technology, Boulder, Colorado 80303

Heterodyne frequency measurements, accurate to 20 kHz, of 35 lines of the 00^02–$[10^01,02^01]_I$ band (10.4 μm) and 33 lines of the 00^02–$[10^01,02^01]_{II}$ band (9.4 μm) of CO_2 have been made with a sequence band CO_2 laser stabilized to line center using the sub-Doppler 4.3-μm fluorescence. A saturated 4.3-μm fluorescence-stabilized regular band CO_2 laser was used as the frequency reference for the heterodyne measurements. New molecular constants were obtained from a least-squares fitting of these new measurements and the previous measurements. Calculated frequency and wavenumber tables for CO_2 sequence band transitions using the new constants are presented. Frequencies of the transitions from the ground state to the 00^02, $[10^01,02^01]_I$, and $[10^01,02^01]_{II}$ levels have been accurately determined to an accuracy of 0.2 MHz by adding the sub-Doppler heterodyne frequency measurements of the $[10^01,02^01]_I$–00^00 transitions made by A. Groh, D. Goddon, M. Schneider, W. Zimmerman, and W. Ubran (*J. Mol. Spectrosc.* **146,** 161–168, 1991).

INTRODUCTION

The sub-Doppler stabilized CO_2 laser has many applications for both high-resolution molecular spectroscopy and secondary frequency and wavelength standards. However, only the regular band CO_2 lasers are often used because saturated 4.3-μm fluorescence stabilization (*1*) is easily applicable to the regular band transitions, and hence their frequencies can be accurately measured (*2, 3*). The range for using this unique spectroscopic laser source is limited by the lack of good stabilization techniques and accurate frequency measurements for the other CO_2 laser bands, such as the 01^11–$[1^110,03^10]_{I,II}$ hot bands and the 00^02–$[10^01,02^01]_{I,II}$ first-sequence bands.

The first frequency measurements of the CO_2 sequence band laser transitions were performed by Siemsen and Whitford in 1977 (*4*). Because their sequence band laser was locked to the peak of the output power, the accuracy of their results was Doppler limited (1–2 MHz). The first sub-Doppler-limited frequency measurement on the sequence band was made in 1990 by Zink *et al.* (*5*); however, only one transition, the $P(33)$ of the 00^02–$[10^01,02^01]_I$ band, was measured. Later Shieh *et al.* (*6*) reported another sub-Doppler-limited determination of frequencies of 19 lines with an accuracy of about 400 kHz. Both groups used the optogalvanic Lamb-dip in an external CO_2 discharge cell to stabilize their sequence band lasers. The main source of uncertainty comes from instabilities in the sequence band lasers. We have recently developed a modified fluorescence scheme (*7*) to stabilize a CO_2 laser oscillating on the first-sequence bands. Compared to optogalvanic Lamb-dip stabilization, this fluorescence

[1] Permanent address: Institute of Physics, Academy of Science of Belarus, Minsk, Belarus.

0022-2852/95 $12.00

stabilization provides a better signal/noise ratio and can operate at a lower CO_2 pressure, reducing the pressure broadening and pressure shift. Using this method, we also stabilized the hot band lasers, including the newly observed 9-μm hot band (*8*), and measured their transition frequencies (*9*).

In this paper we report our heterodyne transition frequency measurements of 00^02–$[10^01,02^01]_{I,II}$ bands of CO_2 using a 4.3-μm fluorescence-stabilized sequence band CO_2 laser. We have used new, more accurate, values of the regular band transition frequencies as reference frequencies (*9*). We achieved an estimated uncertainty of less than 20 kHz for the sequence band transition frequencies. Improved molecular constants were also obtained by the least-squares fitting of new and previous measurements.

EXPERIMENTAL DETAILS

The measurements were performed at both NIST (National Institute of Standards and Technology) and NTHU (National Tsing Hua University, Taiwan, Republic of China) using quite similar techniques. Sixty-eight sequence band lines were measured: 45 at NIST and 26 at NTHU (3 lines were measured at both NIST and NTHU). The scheme of our heterodyne frequency measurements is shown in Fig. 1. The cw sequence band CO_2 lasers that were used in each experiment differ in the method of selecting the sequence band lines.

Sequence band lines can be selected either by placing a hot CO_2 absorption cell inside the cavity of a conventional CO_2 laser (*10*) or by using a laser cavity with special wavelength discrimination (*8, 11, 12*). The NIST high-resolution laser used the second approach; it has a multiribbed tube and a 171 line/mm diffraction grating. This laser has an active discharge length of 1.34 m and uses a flowing gas mixture of 10% CO_2, 12% N_2, and 78% He. The windowless laser cavity consists of a Littrow-mounted grating and a 10-m radius gold coated mirror with a separation of 1.5 m. The zeroth-order reflection of the laser grating is used as the laser output. The laser oscillates on many sequence band lines; however, it was impossible to select those which are close to the regular band lines.

In order to measure the frequency of those lines which the NIST CO_2 laser cannot select, the NTHU measurements used the hot cell method for sequence band line selection. The NTHU gas-flow CO_2 laser, which was used in previous work (*6*), has

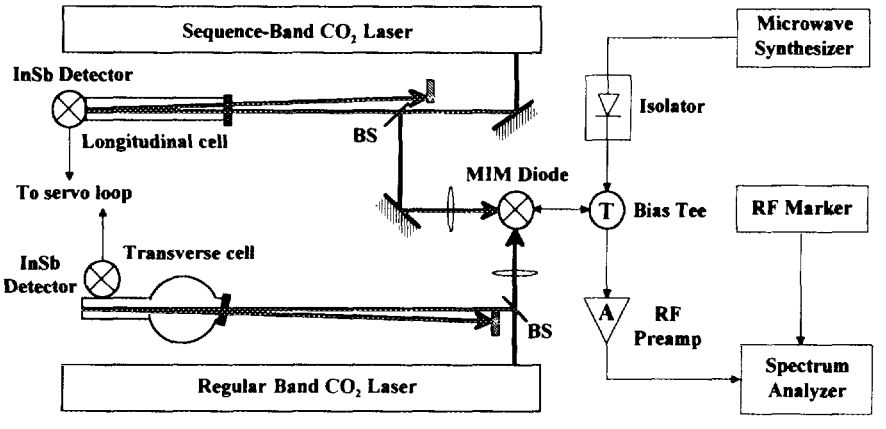

FIG. 1. Experimental setup for the heterodyne frequency measurements.

a 3.65-m cavity length and its cavity consists of a 150-line/mm grating and a 99 or 95% ZnSe output coupler with a 5-m radius of curvature. The total discharge length is 2.3 m. A 0.6-m-long hot cell near the grating is used to suppress the regular band oscillation. With a laser gas mixture of 12% CO_2, 18% N_2, and 70% He, total pressure 1733 Pa (13 Torr) and CO_2 temperature in the hot cell of about 260°C, we are able to obtain more than 1 W for most of the sequence band lines.

A modified 4.3-μm saturated fluorescence stabilization technique is used to stabilize the sequence band CO_2 laser. A discussion of the principle of this technique can be found in Ref. (*7*). Here we briefly describe our operating conditions. We use a longitudinal cell where the detector field of view is located along the laser beam. The cell involves the flow of pure CO_2 heated to 300–380°C at a pressure of 26 Pa (200 mTorr). It utilizes a quartz tube with an internal gold coating. Except for some weak lines, the frequency stability achieved was less than 20 kHz. Our regular-band CO_2 laser uses a conventional, transverse-type, 4.3-μm fluorescence cell filled with a reference CO_2 gas pressure of 5.3 Pa (40 mTorr). Liquid-nitrogen-cooled InSb detectors are used to detect the 4.3-μm fluorescence in both longitudinal and transverse cells.

The reference laser beam as well as the sequence band laser beam are focused onto the point-contact metal–insulator–metal (MIM) diode as shown in Fig. 1. When the difference frequencies are higher than 1 GHz, the beat signals are further down-converted by feeding a microwave frequency to the MIM diode. A synthesized microwave signal generator serves this purpose. The frequency of the microwave is chosen so that the final difference frequency is within the 1-GHz bandwidth of the rf preamplifier. The frequency ν to be determined is then given by

$$\nu = \nu_{\text{ref}} \mp (m\nu_{\text{micr}} \mp \nu_{\text{beat}}), \tag{1}$$

where ν_{ref}, ν_{micr}, and ν_{beat} are the frequencies of the reference laser, microwave, and the resulting beat signal, and m is the harmonic order of the microwave generated in the MIM diode. The output signals were observed using a spectrum analyzer. The frequencies were measured by comparison with a known marker frequency. The signal for the frequency marker was generated by a signal generator which was locked and counted by a microwave frequency counter. This method allows us to decrease the marker readout error to 1 kHz.

The beat frequency was usually averaged for 1 min (30 sec for the NTHU measurements). Typically, five measurements were taken for each sequence band transition (12–16 for the NTHU measurements); each time the laser was carefully locked to the center of the saturation dip. The relative phase and amplitude of the frequency dithers of the two lasers were adjusted to minimize the width of the beat notes to about 600 kHz for each experimental setup.

Before the start of the NTHU measurements a two-step calibration procedure for the measurement section was made. First, we measured the difference frequency between two 00^01–$[10^00,02^00]_{II}$ regular band transitions, the $9R(24)$ and $9R(26)$; second, we measured the frequency of the $9R(9)$, $9R(27)$ and $9P(19)$ lines of the 00^02–$[10^01,02^01]_{II}$ sequence band which had been previously measured at NIST. All these calibration measurements showed good agreement with the new value for the regular band transition frequency (*9*) as well as with the measured values for the sequence band transition frequencies at NIST.

RESULTS

The combined results of the measurements are listed in Tables I and II for the 10.4- and 9.4-μm sequence bands. The standard deviation of the frequency measurement

TABLE I

Observed Beat Frequencies for the $00^02-[10^01,02^01]_{II}$ Laser Band

Seq. Line	Ref. Line[a]	Beat Freq. [MHz]	Uncertainty [MHz]	Obs.-Calc. [MHz]
P(45)	10*P*(46)	-29 282.476	(0.015)	0.000
P(43)	10*P*(44)	-30 297.403	(0.015)	-0.011
P(41)	10*P*(42)	-31 299.105	(0.015)	-0.005
P(39)	10*P*(42)	29 460.373	(0.015)	0.041
P(37)	10*P*(40)	27 724.942	(0.015)	0.000
P(35)	10*P*(38)	26 006.284	(0.015)	-0.016
P(33)	10*P*(36)	24 304.106	(0.018)	-0.002
P(31)	10*P*(34)	22 618.049	(0.015)	-0.020
P(29)	10*P*(32)	20 947.902	(0.016)	0.012
P(27)	10*P*(30)	19 293.267	(0.015)	-0.009
P(25)	10*P*(28)	17 653.953	(0.015)	0.017
P(23)	10*P*(26)	16 029.570	(0.015)	-0.007
P(21)	10*P*(24)	14 419.920	(0.015)	0.011
P(19)	10*P*(22)	12 824.641	(0.015)	0.001
P(17)	10*P*(20)	11 243.478	(0.015)	0.000
P(15)	10*P*(18)	9 676.150	(0.019)	0.018
P(13)	10*P*(16)	8 122.292[b]	(0.015)	-0.017
P(11)	10*P*(14)	6 581.714[b]	(0.015)	0.000
R(5)	10*R*(2)	-6 021.459	(0.015)	-0.003
R(7)	10*R*(4)	-7 451.411	(0.015)	-0.003
R(9)	10*R*(6)	-8 871.352	(0.015)	0.005
R(11)	10*R*(8)	-10 281.639	(0.015)	-0.007
R(13)	10*R*(10)	-11 682.553	(0.015)	0.014
R(15)	10*R*(12)	-13 074.501	(0.016)	0.001
R(17)	10*R*(14)	-14 457.786	(0.015)	-0.002
R(19)	10*R*(16)	-15 832.770	(0.015)	-0.005
R(21)	10*R*(18)	-17 199.798	(0.015)	0.007
R(23)	10*R*(18)	20 668.560	(0.015)	-0.010
R(25)	10*R*(20)	18 566.316	(0.015)	0.014
R(27)	10*R*(22)	16 467.790	(0.015)	-0.005
R(29)	10*R*(24)	14 372.436	(0.015)	0.002
R(31)	10*R*(26)	12 279.584	(0.015)	-0.005
R(33)	10*R*(28)	10 188.614[b]	(0.019)	-0.007
R(35)	10*R*(30)	8 098.866[b]	(0.016)	-0.009
R(37)	10*R*(32)	6 009.730[b]	(0.041)	0.050

[a] The 10 designation before the reference laser transition indicates the 10-μm transition of the $^{12}C^{16}O_2$ laser was used.

[b] Measurements were made at the National Tsing Hua University; the other measurements were made at NIST.

for each line was generally better than 20 kHz (only a few high-J lines have 40–50 kHz deviations). The frequency uncertainty of every sequence band transition is presented in parentheses following the measured beat frequency. The uncertainty assigned to each measurement was increased whenever necessary to ensure that the deviation obtained from the fit was not much larger than the uncertainty.

The main contribution to the systematic error is due to a pressure shift of the CO_2 line center in the fluorescence cell. Line-center shifts of 15 kHz for the sequence band transitions and 3 kHz for reference lines of the regular bands are estimated from the data of Soohoo *et al.* (*13*). Even on the assumption that the pressure shifts have different signs (*13*), the sum is still in the range of the measured uncertainty. Thus from analyzing the measured data we conclude that the measurement accuracy is less than 20 kHz.

Due to an accidental overlapping with one line belonging to another band, we found that the $R(21)$ of $00^02-[10^01,02^01]_{II}$ band has an anomalous 4.3-μm fluorescence

TABLE II

Observed Beat Frequencies for the 00^02–$[10^01,02^01]_{II}$ Laser Band

Seq. Line	Ref. Line[a]	Beat Freq. [MHz]	Uncertainty [MHz]	Obs.-Calc. [MHz]
P(37)	9*P*(40)	-2 260.419[b]	(0.050)	0.004
P(35)	9*P*(38)	-3 324.501[b]	(0.026)	-0.012
P(33)	9*P*(36)	-4 418.636[b]	(0.015)	0.007
P(31)	9*P*(34)	-5 542.693[b]	(0.015)	-0.002
P(29)	9*P*(32)	-6 696.429[b]	(0.015)	-0.005
P(27)	9*P*(30)	-7 879.624[b]	(0.015)	-0.010
P(25)	9*P*(28)	-9 092.026[b]	(0.015)	-0.004
P(23)	9*P*(26)	-10 333.404	(0.015)	-0.016
P(21)	9*P*(24)	-11 603.429	(0.015)	0.011
P(19)	9*P*(22)	-12 901.897	(0.032)	-0.005
P(19)	9*P*(22)	-12 901.886[b]	(0.029)	0.006
P(17)	9*P*(20)	-14 228.420	(0.021)	0.021
P(15)	9*P*(18)	-15 584.755	(0.015)	0.019
P(13)	9*P*(16)	-16 964.556	(0.022)	0.006
P(11)	9*P*(14)	-18 373.465	(0.015)	-0.001
P(9)	9*P*(12)	-19 809.153	(0.020)	-0.026
P(7)	9*P*(10)	-21 271.192	(0.015)	-0.006
R(5)	9*R*(2)	-31 391.015	(0.015)	0.022
R(7)	9*R*(2)	11 982.928[b]	(0.018)	-0.005
R(9)	9*R*(4)	9 510.242[b]	(0.023)	0.003
R(9)	9*R*(4)	9 510.234	(0.015)	-0.005
R(11)	9*R*(6)	7 015.093[b]	(0.015)	-0.011
R(13)	9*R*(8)	4 498.259[b]	(0.015)	-0.005
R(15)	9*R*(10)	1 960.455[b]	(0.018)	-0.004
R(17)	9*R*(12)	-597.562[b]	(0.017)	0.003
R(19)	9*R*(14)	-3 175.066[b]	(0.016)	-0.009
R(23)	9*R*(18)	-8 385.425[b]	(0.025)	0.009
R(25)	9*R*(20)	-11 016.782[b]	(0.022)	0.023
R(27)	9*R*(22)	-13 664.613[b]	(0.015)	0.005
R(27)	9*R*(22)	-13 664.697	(0.031)	-0.079
R(29)	9*R*(24)	-16 328.103	(0.015)	0.013
R(31)	9*R*(24)	17 232.726	(0.015)	0.017
R(33)	9*R*(26)	13 752.537	(0.015)	-0.009

[a] The 9 designation before the reference laser transition indicates the 9-μm transition of the $^{12}C^{16}O_2$ laser was used.

[b] Measurements were made at the National Tsing Hua University; the other measurements were made at NIST.

signal profile. Such overlappings are also reported for some regular and hot band lines (*14*). A literature search for possible candidates shows that the transition frequency of the $R(35)$ line of the $[11^11,03^11]_I$–$[21^10,13^10,05^10]_{II}$ band is very close to the transition frequency of this sequence band line. Preliminary calculations using data from Rothman (*15*) predicted that the frequency of the $R(35)$ is about 32 MHz higher than that of the 9-μm $R(21)$ sequence line. Moreover, the energy level of the $[21^10,13^10,05^10]_{II}$ state is 300 cm^{-1} lower than the $[10^01,02^01]_{II}$ state. The absorption of the $9R(21)$ laser line comes from these two transitions, and the maximum of the fluorescence signal profile is obviously blue-shifted away from the saturation dip. The measured transition frequency of the fluorescence-stabilized $9R(21)$ line has a -142 kHz discrepancy from our calculated frequency in Table V and was not included in Table II or in the least-squares fit. Thus, the $9R(21)$ sequence band line cannot be used as a good reference for high-resolution spectroscopy.

Using an acousto-optical modulator, we upshifted the frequency of the sequence band laser by 40 MHz and observed the fluorescence saturation-dip of the $R(35)$ line

TABLE III

Constants (in MHz) for the First Sequence Band Laser Transitions of CO_2

constant	this work	Ref. (19)	Ref. (17)	Ref. (18)
$00^02-[10^01,02^01]_I$				
ν_0	28 736 412.218 4(72)[a]			
B'	11 514.013 441 8(1058)		11 514.015(2)	
$D'\times10^3$	3.978 312 72(7105)		3.977 4(6)	
$H'\times10^{10}$	4.538 519(89772)		3.9(6)	
B''	11 603.862 221 8(1066)	11 603.887(9)		11 603.802(15)
$D''\times10^3$	3.426 278 65(7843)	3.436(6)		3.387(6)
$H''\times10^{10}$	58.723 628(162092)	75.(6)		---
$00^02-[10^01,02^01]_{II}$				
ν_0	31 792 530.830 8(84)			
B'	11 514.013 441 8(1058)		11 514.015(2)	
$D'\times10^3$	3.978 312 72(7105)		3.977 4(6)	
$H'\times10^{10}$	4.538 519(89772)		3.9(6)	
B''	11 617.053 471 1(1221)	11 617.042(12)		11 617.007(15)
$D''\times10^3$	4.724 170 83(14591)	4.713(6)		4.690(6)
$H''\times10^{10}$	67.973 706(675883)	51.(6)		---

[a] The uncertainty (one standard deviation) in the last digit is given in parentheses. More digits are given than the uncertainty would warrant in order to allow for correlation among the constants.

of the $[11^11,03^11]_I$–$[21^10,13^10,05^10]_{II}$ band. The measured transition frequency of this line was 32 251 570. 645(0.014) MHz which is 38.6 MHz higher than the frequency of the $9R(21)$ sequence band line. Since only one line was measured, we cannot determine the constants of the $[11^1,03^1]_I$–$[21^10,13^10,05^10]_{II}$ band.

ANALYSIS

The experimental data shown in Tables I and II were used in a least-squares fitting to obtain new rovibrational constants for 00^02–$[10^01,02^01]_{I,II}$ sequence bands. The present measurements were combined with the earlier heterodyne frequency measurements of sequence band transitions by Siemsen and Whitford (*4*) and Shieh *et al.* (*6*). The one measurement of Zink *et al.* (*5*) was also included in the fit. Groh *et al.* (*16*) have made sub-Doppler heterodyne frequency measurements on the $[10^01,02^01]_I$–00^00 transition by using a stabilized CO laser as a frequency standard.

No frequency measurements have been made for $J > 46$. To ensure that the most poorly determined constants H_v do not badly distort the calculated values, we have

TABLE IV

Frequency Separation of the Sequence-Laser Levels from the Ground State and Ground State Constants Resulting from the Present Fit

$\nu_0(00^02-00^00)$	= 140 102 769.78(23)[a]MHz	= 4673.325 363(7) cm^{-1}
$\nu_0([10^01,02^01]_I-00^00)$	= 111 366 357.56(23) MHz	= 3714.781 829(7) cm^{-1}
$\nu_0([10^01,02^01]_{II}-00^00)$	= 108 310 238.94(23) MHz	= 3612.840 685(7) cm^{-1}
B_0	= 0.390 218 956 0(192) cm^{-1}	
D_0	= 1.333 746(60)$\times10^{-7}$ cm^{-1}	
H_0	= 1.330(52)$\times10^{-14}$ cm^{-1}	

[a] The uncertainty in the last digits is given in parentheses.

TABLE V

Calculated Frequency for the 00^02–$[10^01,02^01]_I$ and 00^02–$[10^01,02^01]_{II}$ Bands of $^{12}C^{16}O_2$ with the Estimated 1-σ Uncertainties

Line	10-μm Band Frequency (MHz)	Uncertainty (MHz)	Line	9-μm Band Frequency (MHz)	Uncertainty (MHz)
P(55)	27 190 387.559	0.110	P(55)	30 218 162.421	0.964
P(53)	27 256 498.803	0.076	P(53)	30 285 473.467	0.726
P(51)	27 321 830.274	0.051	P(51)	30 352 076.651	0.536
P(49)	27 386 387.529	0.032	P(49)	30 417 964.575	0.388
P(47)	27 450 175.832	0.019	P(47)	30 483 130.033	0.274
P(45)	27 513 200.155	0.011	P(45)	30 547 566.015	0.187
P(43)	27 575 465.191	0.007	P(43)	30 611 265.712	0.123
P(41)	27 636 975.353	0.006	P(41)	30 674 222.529	0.077
P(39)	27 697 734.785	0.006	P(39)	30 736 430.087	0.046
P(37)	27 757 747.363	0.006	P(37)	30 797 882.228	0.025
P(35)	27 817 016.704	0.005	P(35)	30 858 573.026	0.012
P(33)	27 875 546.168	0.005	P(33)	30 918 496.788	0.007
P(31)	27 933 338.863	0.004	P(31)	30 977 648.062	0.006
P(29)	27 990 397.650	0.004	P(29)	31 036 021.641	0.006
P(27)	28 046 725.148	0.004	P(27)	31 093 612.568	0.005
P(25)	28 102 323.735	0.004	P(25)	31 150 416.141	0.005
P(23)	28 157 195.554	0.004	P(23)	31 206 427.914	0.005
P(21)	28 211 342.516	0.004	P(21)	31 261 643.708	0.005
P(19)	28 264 766.302	0.004	P(19)	31 316 059.605	0.006
P(17)	28 317 468.367	0.004	P(17)	31 369 671.960	0.005
P(15)	28 369 449.941	0.004	P(15)	31 422 477.400	0.005
P(13)	28 420 712.033	0.005	P(13)	31 474 472.824	0.005
P(11)	28 471 255.433	0.005	P(11)	31 525 655.413	0.005
P(9)	28 521 080.712	0.006	P(9)	31 576 022.624	0.005
P(7)	28 570 188.225	0.006	P(7)	31 625 572.197	0.006
P(5)	28 618 578.113	0.007	P(5)	31 674 302.156	0.007
P(3)	28 666 250.303	0.007	P(3)	31 722 210.807	0.008
P(1)	28 713 204.508	0.007	P(1)	31 769 296.743	0.008
R(1)	28 782 288.445	0.007	R(1)	31 838 380.680	0.008
R(3)	28 827 445.043	0.007	R(3)	31 883 405.547	0.008
R(5)	28 871 880.982	0.006	R(5)	31 927 605.025	0.007
R(7)	28 915 595.022	0.006	R(7)	31 970 978.995	0.006
R(9)	28 958 585.709	0.005	R(9)	32 013 527.621	0.005
R(11)	29 000 851.374	0.004	R(11)	32 055 251.354	0.005
R(13)	29 042 390.134	0.004	R(13)	32 096 150.925	0.005
R(15)	29 083 199.892	0.004	R(15)	32 136 227.360	0.005
R(17)	29 123 278.329	0.004	R(17)	32 175 481.922	0.006
R(19)	29 162 622.911	0.004	R(19)	32 213 916.214	0.006
R(21)	29 201 230.881	0.004	R(21)	32 251 532.072	0.006
R(23)	29 239 099.256	0.004	R(23)	32 288 331.816	0.005
R(25)	29 276 224.829	0.004	R(25)	32 324 317.235	0.005
R(27)	29 312 604.164	0.004	R(27)	32 359 491.584	0.005
R(29)	29 348 233.592	0.004	R(29)	32 393 857.583	0.006
R(31)	29 383 109.209	0.005	R(31)	32 427 418.408	0.006
R(33)	29 417 226.870	0.006	R(33)	32 460 177.490	0.008
R(35)	29 450 582.191	0.008	R(35)	32 492 138.513	0.014
R(37)	29 483 170.538	0.009	R(37)	32 523 305.403	0.026
R(39)	29 514 987.027	0.012	R(39)	32 553 682.329	0.047
R(41)	29 546 026.518	0.014	R(41)	32 583 273.694	0.079
R(43)	29 576 283.610	0.018	R(43)	32 612 084.132	0.125
R(45)	29 605 752.638	0.023	R(45)	32 640 118.498	0.189
R(47)	29 634 427.664	0.031	R(47)	32 667 381.868	0.276
R(49)	29 662 302.477	0.043	R(49)	32 693 879.523	0.390
R(51)	29 689 370.579	0.061	R(51)	32 719 616.956	0.539
R(53)	29 715 625.188	0.086	R(53)	32 744 599.852	0.729

also included in the fit the Fourier transform measurements of Bailly *et al.* (*17*) for the 00^02–00^01 band which extends to $J = 92$. Those measurements aid in the determination of the rotational and centrifugal distortion constants but they do not contribute to the determination of the band centers for the laser transitions.

The least-squares fit of the transitions uses the equations

$$E = G_v + B_v[J(J+1)] - D_v[J(J+1)]^2 + H_v[J(J+1)]^3, \tag{2}$$

and

$$\nu_0 = G'_v - G''_v. \tag{3}$$

The observed transitions are then given by

$$\nu_{obs} = E' - E''. \tag{4}$$

TABLE VI

Calculated Wavenumbers for the 00^02–$[10^01,02^01]_I$ and 00^02–$[10^01,02^01]_{II}$ Bands of $^{12}C^{16}O_2$ with the Estimated 1-σ Uncertainties

Line	10-μm Band Wavenumber(Unc)[a] (cm^{-1})	Line	9-μm Band Wavenumber(Unc) (cm^{-1})
P(55)	906.973 702 4(37)	P(55)	1007.969 400 6(322)
P(53)	909.178 936 2(25)	P(53)	1010.214 655 5(242)
P(51)	911.358 159 5(17)	P(51)	1012.436 298 5(179)
P(49)	913.511 557 7(11)	P(49)	1014.634 083 1(129)
P(47)	915.639 306 4(7)	P(47)	1016.807 768 8(91)
P(45)	917.741 571 6(4)	P(45)	1018.957 121 8(62)
P(43)	919.818 509 6(2)	P(43)	1021.081 915 0(41)
P(41)	921.870 267 8(2)	P(41)	1023.181 928 4(26)
P(39)	923.896 984 2(2)	P(39)	1025.256 949 2(15)
P(37)	925.898 788 4(2)	P(37)	1027.306 771 9(8)
P(35)	927.875 800 8(2)	P(35)	1029.331 199 0(4)
P(33)	929.828 133 6(2)	P(33)	1031.330 040 6(2)
P(31)	931.755 890 4(2)	P(31)	1033.303 114 7(2)
P(29)	933.659 166 6(1)	P(29)	1035.250 247 7(2)
P(27)	935.538 049 7(1)	P(27)	1037.171 274 3(2)
P(25)	937.392 619 0(1)	P(25)	1039.066 037 5(2)
P(23)	939.222 945 8(1)	P(23)	1040.934 389 2(2)
P(21)	941.029 094 1(1)	P(21)	1042.776 189 8(2)
P(19)	942.811 119 8(1)	P(19)	1044.591 308 7(2)
P(17)	944.569 071 4(1)	P(17)	1046.379 624 4(2)
P(15)	946.302 990 1(1)	P(15)	1048.141 024 3(2)
P(13)	948.012 909 4(2)	P(13)	1049.875 404 9(2)
P(11)	949.698 855 8(2)	P(11)	1051.582 672 3(2)
P(9)	951.360 848 2(2)	P(9)	1053.262 741 6(2)
P(7)	952.998 898 5(2)	P(7)	1054.915 537 5(2)
P(5)	954.613 011 4(2)	P(5)	1056.540 994 0(2)
P(3)	956.203 184 5(2)	P(3)	1058.139 054 6(3)
P(1)	957.769 408 2(2)	P(1)	1059.709 672 3(3)
R(1)	960.073 800 3(2)	R(1)	1062.014 064 4(3)
R(3)	961.580 062 3(2)	R(3)	1063.515 932 3(3)
R(5)	963.062 285 6(2)	R(5)	1064.990 268 2(2)
R(7)	964.520 429 1(2)	R(7)	1066.437 068 1(2)
R(9)	965.954 444 0(2)	R(9)	1067.856 337 5(2)
R(11)	967.364 274 8(2)	R(11)	1069.248 091 4(2)
R(13)	968.749 858 8(1)	R(13)	1070.612 354 3(2)
R(15)	670.111 125 7(1)	R(15)	1071.949 159 9(2)
R(17)	971.447 998 5(1)	R(17)	1073.258 551 5(2)
R(19)	972.760 392 5(1)	R(19)	1074.540 581 5(2)
R(21)	974.048 215 7(1)	R(21)	1075.795 311 4(2)
R(23)	975.311 368 8(1)	R(23)	1077.022 812 1(2)
R(25)	976.549 744 6(1)	R(25)	1078.223 163 1(2)
R(27)	977.763 228 6(1)	R(27)	1079.396 453 2(2)
R(29)	978.951 698 4(1)	R(29)	1080.542 779 5(2)
R(31)	980.115 023 7(2)	R(31)	1081.662 248 1(2)
R(33)	981.253 066 4(2)	R(33)	1082.754 973 5(3)
R(35)	982.365 680 2(3)	R(35)	1083.821 078 4(5)
R(37)	983.452 710 4(3)	R(37)	1084.860 694 0(9)
R(39)	984.513 994 2(4)	R(39)	1085.873 959 1(16)
R(41)	985.549 360 2(5)	R(41)	1086.861 020 8(26)
R(43)	986.558 628 2(6)	R(43)	1087.822 033 6(42)
R(45)	987.541 609 1(8)	R(45)	1088.757 159 4(63)
R(47)	988.498 105 1(10)	R(47)	1089.666 567 5(92)
R(49)	989.427 908 7(14)	R(49)	1090.550 434 2(130)
R(51)	990.330 803 4(20)	R(51)	1091.408 942 5(180)
R(53)	991.206 562 9(29)	R(53)	1092.242 282 2(243)

[a] The uncertainty in the last digits is given in parentheses.

All of the heterodyne frequency calculations are based on the latest values for the CO_2 laser frequencies (*9*). The least-squares fit used to determine the constants given in Table III and used for calculating the laser transition frequencies given in Tables V and VI is the same as the fit used in Ref. (*9*), except that these transitions are added to the database. For the heterodyne measurements, only the frequency differences (from the regular CO_2 laser transitions) are used in the fit.

The constants resulting from this fit are given in Table III and compared with the constants determined by earlier FTS measurements (*17–19*). Table IV gives the absolute value of the frequencies, with respect to the ground state, of the three vibrational energy levels involved in the laser transitions. Table IV also gives the rotational constants for the ground state as determined by the present fit.

The present constants are in good agreement with the earlier determinations, including the constants given by Siemsen and Whitford (*4*), but are much more accurate. These new measurements, when coupled with the frequency measurements of Groh *et al.* (*16*), give frequencies of the transitions from the ground state to the 00^02, $[10^01,02^01]_I$, and $[10^01,02^01]_{II}$ levels that have absolute uncertainties on the order of 0.2 MHz (0.000007 cm^{-1}).

Tables V and VI give the calculated values for the first sequence band laser transitions. The uncertainties given in Tables V and VI are calculated from the variance–covariance matrix elements given by the least-squares fit.

CONCLUSIONS

With the sequence band laser stabilized to the saturation dip of the 4.3-μm fluorescence, we measured the frequencies of 68 00^02–$[10^01,02^01]_{I,II}$ sequence band transitions. The frequencies of the fluorescence-stabilized sequence band lasers are now known within 20 kHz accuracy. We also obtained accurate molecular constants by a least-squares fit of the data of all of the new measurements. $9R(21)$ cannot be used as a reference due to the overlapping with the $R(35)$ line of the $[11^11,03^11]_I$–$[21^10,13^10,05^10]_{II}$ band. In addition, the frequency of $R(35)$ of the $[11^1,03^11]_I$–$[21^10,13^10,05^10]_{II}$ band was determined accurately. The frequency stability and reproducibility of the fluorescence-stabilized, sequence-band laser enhance its use for either high-resolution spectroscopy or precision calibration bench marks in heterodyne spectroscopy. By coupling with the sub-Doppler heterodyne frequency measurements of the $[10^01,02^01]_I$–00^00 transitions, we can accurately determine the absorption frequencies of the transitions from the ground state to the 00^02, $[10^01,02^01]_I$, and $[10^01,02^01]_{II}$ levels to an accuracy of ± 0.2 MHz as well as the rotational constants of the ground state.

ACKNOWLEDGMENTS

Che-Chung Chou is extremely grateful to the Ministry of Education, Republic of China, for providing the funds for his stay at NIST. This work was partially supported by National Science Council of the Republic of China under Grant NSC 83-0417-M-007-032.

RECEIVED: February 1, 1995

REFERENCES

1. C. FREED AND A. JAVAN, *Appl. Phys. Lett.* **17**, 53–56 (1970).
2. F. R. PETERSEN, E. C. BEATY, AND C. R. POLLOCK, *J. Mol. Spectrosc.* **102**, 112–122 (1983).
3. L. C. BRADLEY, K. L. SOOHOO, AND C. FREED, *IEEE J. Quantum Electron.* **22**, 234–267 (1986).
4. K. J. SIEMSEN AND B. G. WHITFORD, *Opt. Commun.* **22**, 11–16 (1977).
5. L. ZINK, F. S. PAVONE, R. MEUCCI, M. PREVEDELLI, AND M. INGUSCIO, *Opt. Commun.* **77**, 41–44 (1990).
6. C.-Y. SHIEH, C.-C. CHOU, C.-C. CHEN, T.-M. HUANG, J.-D. CHERN, T.-C. YEN, AND J.-T. SHY, *Opt. Commun.* **88**, 47–53 (1992).
7. C.-C. CHOU, J.-T. SHY, AND T.-C. YEN, *Opt. Lett.* **17**, 967–969 (1992).
8. K. M. EVENSON, C.-C. CHOU, B. W. BACH, AND K. G. BACH, *IEEE J. Quantum Electron.* **30**, 1187–1188 (1994).
9. A. G. MAKI, C.-C. CHOU, K. M. EVENSON, L. R. ZINK, AND J.-T. SHY, *J. Mol. Spectrosc.* **167**, 211–224 (1994).
10. J. REID AND K. SIEMSEN, *J. Appl. Phys.* **48**, 2712–2717 (1977).
11. V. P. AVTONOMOV, V. N. BEL'TUGOV, A. A. KUZNETSOV, V. N. OCHKIN, N. N. SOBOLEV, M. V. SPIRIDONOV, YU. V. TROITSKII, AND B. YU. UDALOV, *Sov. J. Quantum Electron.* **12**, 1400–1408 (1982).

12. A. S. SOLODUKHIN, *J. Mod. Opt.* **34,** 577–580 (1987).
13. K. L. SOOHOO, C. FREED, J. E. THOMAS, AND H. A. HAUS, *IEEE J. Quantum Electron.* **21,** 1159–1171 (1985).
14. B. G. WHITFORD, K. I. SIEMSEN, AND J. REID, *Opt. Commun.* **22,** 261–264 (1977).
15. L. S. ROTHMAN, *Appl. Opt.* **25,** 1795–1816 (1986).
16. A. GROH, D. GODDON, M. SCHNEIDER, W. ZIMMERMANN, AND W. UBRAN, *J. Mol. Spectrosc.* **146,** 161–168 (1991).
17. D. BAILLY, R. FARRENQ, G. GUELACHVILI, AND C. ROSSETTI, *J. Mol. Spectrosc.* **90,** 74–105 (1981).
18. D. BAILLY, *J. Mol. Spectrosc.* **161,** 275–283 (1993).
19. D. BAILLY AND C. ROSSETTI, *J. Mol. Spectrosc.* **102,** 392–398 (1983).